Inorganic Chemistry

ARTICLE

pubs.acs.org/IC

A Heterobimetallic Ruthenium−Gadolinium Complex as a Potential Agent for Bimodal Imaging

Geert Dehaen,[†] Peter Verwilst,[†] Svetlana V. Eliseeva,[†] Sophie Laurent,[‡] Luce Vander Elst,[‡] Robert N. Muller,[‡] Wim M. De Borggraeve,[†] Koen Binnemans,[†] and Tatjana N. Parac-Vogt*[,†]

[†]Department of Chemistry, Katholieke Universiteit Leuven, Celestijnenlaan 200F, P.O. Box 2404, B-3001 Heverlee, Belgium

[‡]NMR and Molecular Imaging Laboratory, Department of General, Organic and Biomedical Chemistry, University of Mons-Hainaut, 7000 Mons, Belgium

Supporting Information

ABSTRACT: Trinuclear heterobimetallic $Ln^{III}-Ru^{II}$ complexes (Ln = Eu, Gd) based on a 1,10-phenanthroline ligand bearing a diethylenetriaminepentaacetic acid (DTPA) core have been synthesized and fully characterized by a range of experimental techniques. The ^{17}O NMR and proton nuclear magnetic relaxation dispersion (NMRD) measurements of $Gd^{III}-Ru^{II}$ show that, in comparison to the parent Gd-DTPA, this complex exhibits improved relaxivity, which is the result of an increase of the rotational correlation time. Relaxometry and ultrafiltration experiments indicate that the 1,10-phenanthroline ligand has a high affinity for noncovalent binding to human serum albumin, which results in a high relaxivity r_1 of 14.3 s^{-1} mM^{-1} at 20 MHz and 37 °C. Furthermore, the $Ln^{III}-Ru^{II}$ complexes (Ln = Eu, Gd) show an intense light absorption in the visible spectral region due to metal-to-ligand charge transfer (MLCT) transitions. Upon excitation into the MLCT band at 440 nm, the complexes exhibit a bright-red luminescence centered at 610 nm, with a quantum yield of 4.7%. The luminescence lifetime equals 540 ns and is therefore long enough to exceed the fluorescent background. Monometallic lanthanide complexes have also been synthesized, and the Eu^{III} analogue shows a characteristic red luminescence with a quantum yield of 0.8%. Taking into account the relaxometric and luminescent properties, the developed $Gd^{III}-Ru^{II}$ complex can be considered as a potential in vitro bimodal imaging agent.

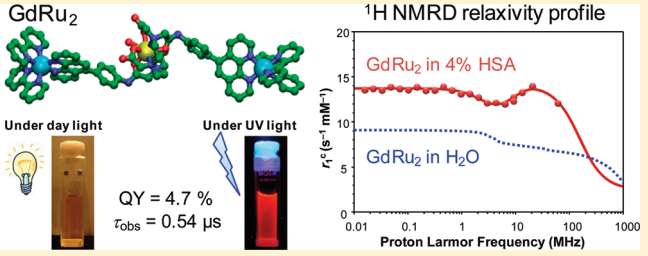

INTRODUCTION

In the search for the development of new, promising contrast agents, multimodal imaging agents are gaining nowadays great attention in the field of clinical and preclinical imaging applications. Powerful in vivo techniques such as magnetic resonance imaging (MRI), positron emission tomography, single-photon emission tomography, and computed tomography are ubiquitous in clinical diagnostics and research centers. Because each imaging technique has its own strengths and weaknesses, the combination of different, complementary techniques can overcome inherent limitations that are associated with one individual technique.[1−4] Whereas MRI is ideal for whole body images because of its good spatial resolution,[5] its sensitivity is rather low so that millimolar concentrations of Gd^{III}-based contrast agents are required. Luminescence-based imaging, on the other hand, can provide high-resolution images, but this technique is only suitable for thin tissue samples because of the low optical transparency of biological tissue.[6−8] Because biological samples strongly absorb at UV and visible wavelengths, suitable metal complexes for luminescence-based imaging are restricted to those showing emission in the red end of the visible spectrum and in the near-infrared (NIR) because radiation of these wavelengths can more easily and effectively penetrate tissues.[9] Long-lived luminescence from lanthanide ions or transition metals makes them ideal as probes for time-gated luminescence-based imaging.[10−12]

Several approaches to developing potential bimodal imaging agents are already known. A mixture of a Gd^{III} and Eu^{III} complex coordinated by a single ligand has been described where the Gd^{III} chelate acts as a T_1 agent for MRI visualization, while the Eu^{III} chelate acts as a reporter in fluorescence microscopy.[13,14] To obtain a lower concentration of the imaging agent in vivo, several complexes containing an optical entity covalently bound to an MRI agent have been reported. In the majority of the examples, the optical entity is a fluorescent dye[4,8,15,16] or a transition-metal complex.[8,17] More recently, functionalized nanoparticles based on iron oxide (Fe_3O_4),[18] gadolinium oxide (Gd_2O_3) doped with rare earths,[19] and quantum dots[20] have been used as bimodal agents.

Because of their unique photochemical and photophysical properties, Ru^{II} complexes (especially with polypyridine ligands) have been extensively studied and widely used in a variety of different applications.[12,21−25] Ru^{II} complexes possess excellent light-harvesting properties, have relatively long-lived metal-to-ligand

Received: April 8, 2011
Published: September 13, 2011

Scheme 1. Synthesis of Ligand DTPA(ph-phen)$_2$[a]

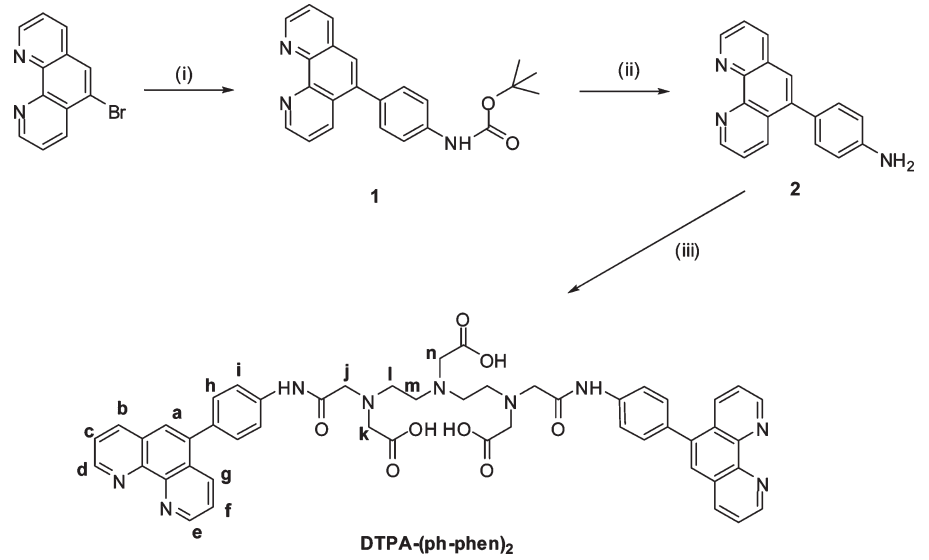

[a] Reaction conditions: (i) *tert*-butyl [4-(4,4,5,5-tetramethyl-1,3,2-dioxaborolan-2-yl)phenyl]carbamate, Cs_2CO_3, $Pd(PPh_3)_4$, reflux, 16 h; (ii) TFA, room temperature, overnight; (iii) DTPA-BA, 60 °C, overnight.

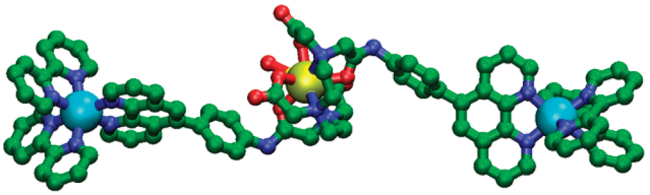

Figure 1. Framework molecular model of the $[\{Ru(bpy)_2\}_2Gd\{DTPA\text{-}(ph\text{-}phen)_2\}(H_2O)]Cl_4$ complex. Hydrogen atoms have been omitted for clarity.

charge transfer (MLCT) states, and show intense luminescence at the red end of the visible spectrum. Taking advantage of these properties, Ru^{II} complexes have been used as sensitizers of NIR emission of Ln ions, such as Yb^{III} and Nd^{III}, in f−d heterometallic diads.[26−30] To explore the application of Ru^{II} compounds in biology, they also have been tested as oxygen sensors,[31] DNA intercalators,[32−34] anticancer agents[35−38] and cell imaging probes.[12]

Although multimodal imaging agents are developing at a growing pace,[3] reports dealing with the design of f−d heterometallic systems for this purpose remain quite scarce. In 2008, Faulkner and co-workers described a bimetallic complex containing a luminescent Re^{I} chromophore bound to an MRI-active Gd^{III}-DOTA derivative.[8] The discovery of a new class of f−d metal systems, so-called *metallostars*,[39,40] has led to the design of a complex with six Ln^{III}-DTTA moieties attached to a single Ru^{II} center.[17] The $Gd^{III}-Ru^{II}$ analogues of such heptametallic species have shown the capability to act as MRI contrast agents, while the $Eu^{III}-Ru^{II}$ complexes display interesting luminescent properties.

In this paper, we report the synthesis of a new f−d heteropolymetallic complex, $[\{Ru(bpy)_2\}_2Ln\{DTPA(ph\text{-}phen)_2\}(H_2O)]Cl_4$ (Ln = Gd, Eu), built by a 1,10-phenanthroline derivative coupled to diethylenetriaminepentaacetic acid bisanhydride (DTPA-BA) suitable for in vitro studies (Scheme 1 and Figure 1). The DTPA-BA arms can coordinate to the Ln^{III} ions, while 1,10-phenanthroline as a soft base is perfectly suited for coordination to Ru^{II}. The relaxometric and luminescent properties of $[\{Ru(bpy)_2\}_2Gd\{DTPA(ph\text{-}phen)_2\}(H_2O)]Cl_4$, as well as its ability to bind to human serum albumin (HSA), have been studied in detail. In addition, monometallic complexes, $[Ln\{DTPA(ph\text{-}phen)_2\}(CH_3OH)]$ (Ln = Gd, Eu), have been synthesized, and the photophysical properties of the Eu^{III} analogue have been investigated in order to gain information about the coordination environment and solvation numbers of the Ln^{III} ions.

RESULTS AND DISCUSSION

Ligand and Complexes. Suzuki cross-coupling of 5-bromo-1,10-phenanthroline with *tert*-butyl [4-(4,4,5,5-tetramethyl-1,3,2-dioxaborolan-2-yl)phenyl]carbamate in the presence of Cs_2CO_3 and $Pd(PPh_3)_4$ in a water/toluene mixture (1:1, v/v) yielded the Boc-protected aniline (**1**), which upon deprotection by trifluoroacetic acid (TFA) gives compound **2**. The reaction of **2** with diethylenetriaminepentaacetic acid bisanhydride (DTPA-BA) in *N*,*N*-dimethylformamide (DMF) overnight at 60 °C yielded the final ligand, $DTPA(ph\text{-}phen)_2$. The free ligand was characterized by ^1H NMR (see Figure S1 in the Supporting Information and Scheme 1 for labeling) and ^{13}C NMR in DMSO-d_6, as well as by two-dimensional COSY NMR (Figure S2 in the Supporting Information).

The electrospray ionization mass spectrometry (ESI-MS) spectrum of the ligand in the negative mode shows the molecular ion peaks corresponding to $[M - H]^-$ at m/z 898.3. The lanthanide complexes $[Ln\{DTPA(ph\text{-}phen)_2\}(CH_3OH)]$ (Ln = Eu, Gd) were obtained by reacting the corresponding lanthanide(III) triflate with ligand $DTPA(ph\text{-}phen)_2$ in methanol (MeOH) in an equimolar ratio. The removal of free Ln ions from the reaction mixture was performed using Chelex 100. The solution was checked with an arsenazo indicator solution, which confirmed the complete removal of free Ln ions.[41] Positive-mode ESI-MS of the complexes shows molecular ion peaks for $[M + Na]^+$ at m/z 1072.9 corresponding to

dx.doi.org/10.1021/ic200726t |*Inorg. Chem.* 2011, 50, 10005–10014

Scheme 2. Synthesis of the $Ln^{III}-Ru^{II}$ $[\{Ru(bpy)_2\}_2Ln\{DTPA(ph\text{-}phen)_2\}(H_2O)]Cl_4$ (Ln = Eu, Gd) Complexes

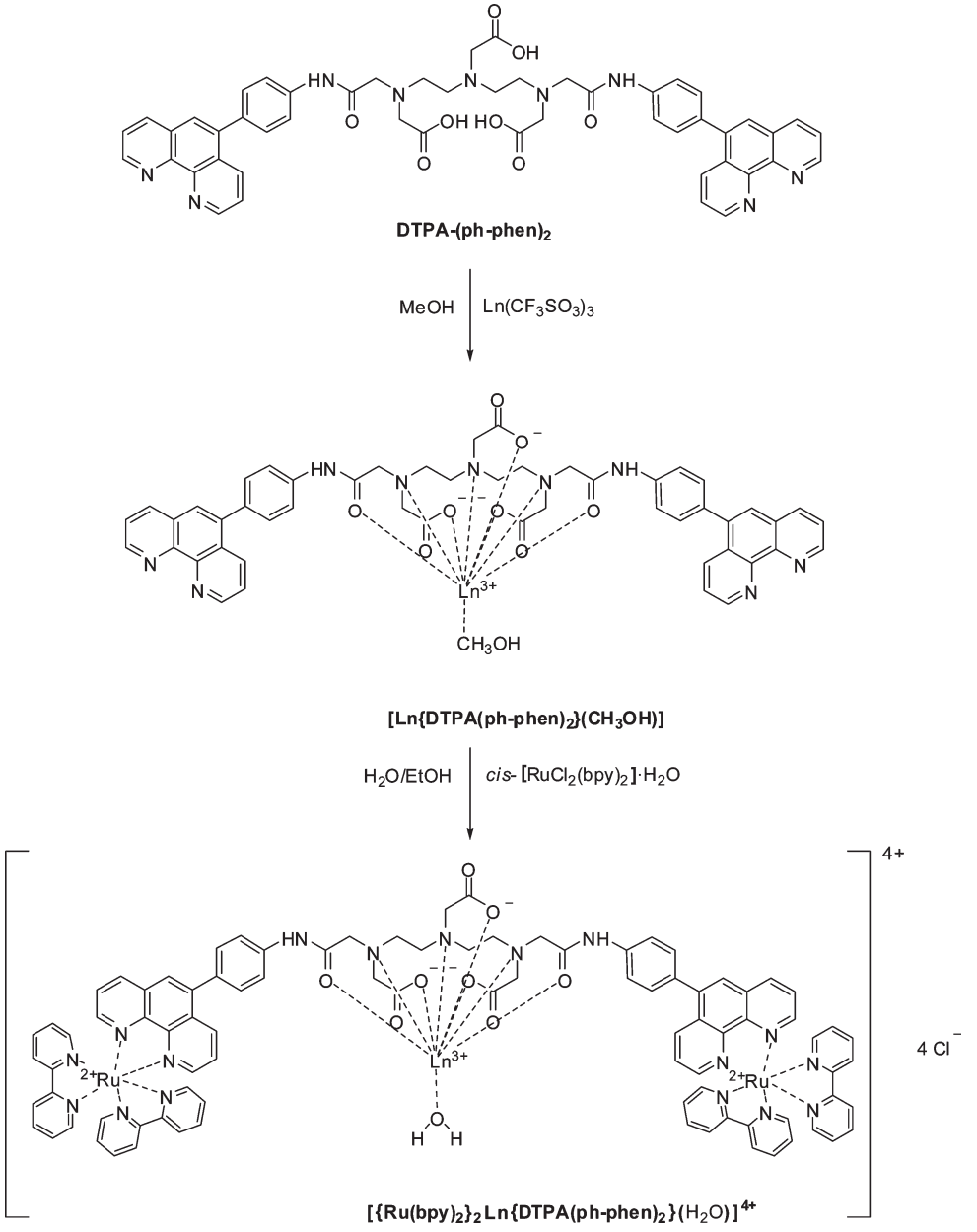

the Eu^{III} complex and those for $[M + 2H]^{2+}$ at m/z 527.9 corresponding to the Gd^{III} complex.

The final complex, $[\{Ru(bpy)_2\}_2Ln\{DTPA(ph\text{-}phen)_2\}(H_2O)]Cl_4$, was obtained by reacting $[Ln\{DTPA(ph\text{-}phen)_2\}(CH_3OH)]$ with *cis*-$[RuCl_2(bpy)_2]$ in a water/ethanol (1:1, v/v) mixture (Scheme 2). The $Ru^{II}-Ln^{III}$ complexes were purified by semipreparative reversed-phase high-performance liquid chromatography (HPLC), resulting in a red solid. The formation of a trinuclear complex, where two Ru^{II} ions are coordinated to 1,10-phenanthroline moieties and one Ln^{III} ion is bound to a DTPA part, is confirmed by HPLC (Figure S3 in the Supporting Information), and ESI-MS shows molecular peaks $[M + 3H_2O]^{4+}$ at m/z 483.2 and 483.3, corresponding to the $Eu^{III}-Ru^{II}$ and $Gd^{III}-Ru^{II}$ complexes, respectively.

Relaxometric Studies. The water proton relaxivity, defined as the paramagnetic longitudinal relaxation rate in reciprocal seconds measured in a solution of Gd^{III} with a concentration of 1 mM, can be characterized by four parameters: the number of water molecules in the first coordination sphere of Gd^{III} (q), the residence time of the coordinated water molecule (τ_M), the relaxation behavior of the electron spin of Gd^{III} (τ_{S1} and τ_{S2}), and the rotational diffusion of the complex in solution (τ_R). The residence time of the coordinated water molecule (τ_M) can be obtained by analysis of the temperature dependence of the reduced transverse relaxation rate of the ^{17}O NMR resonance of water in solutions of the Gd^{III} complex (Figure 2).[42−45] The data obtained in the temperature range 295−354 K show that the exchange rate is in the slow-to-intermediate regime. The parameters related to the electronic relaxation have to be considered with caution.

A theoretical treatment of the experimental data was performed assuming the presence of one water molecule in the first

dx.doi.org/10.1021/ic200726t |*Inorg. Chem.* 2011, 50, 10005–10014

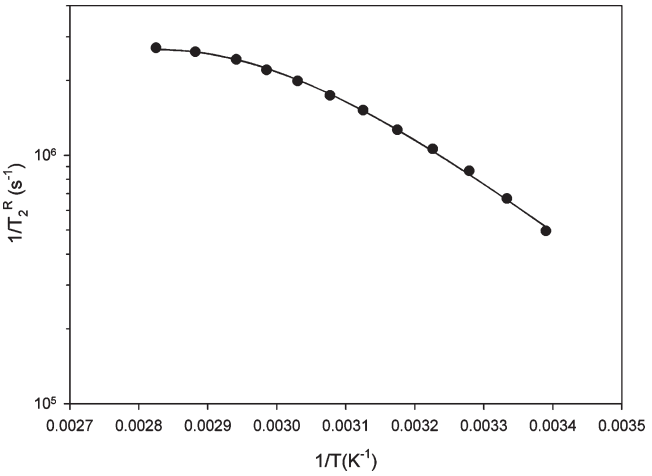

Figure 2. Evolution of the reduced ^{17}O transverse relaxation rate ($1/T_2^R = 55.55/T_2^{para}$[Gd]) versus the reciprocal of the temperature for $[\{Ru(bpy)_2\}_2Gd\{DTPA(ph\text{-}phen)_2\}(H_2O)]Cl_4$ ([Gd] = 6.81 mM).

Table 1. Parameters Obtained by the Theoretical Adjustment of the ^{17}O Transverse Relaxation Rates versus the Reciprocal of the Temperature

	$[\{Ru(bpy)_2\}_2Gd\{DTPA(ph\text{-}phen)_2\}(H_2O)]Cl_4$	Gd-DTPA-BMA[48]
τ_M^{310} (ns)	808 ± 34	967 ± 36
$\Delta H^{\ddagger}$ (kJ mol^{-1})	37.8 ± 0.1	48.0 ± 0.1
$\Delta S^{\ddagger}$ (J mol^{-1} K^{-1})	−6.4 ± 0.2	24.9 ± 0.2
$A/\hbar$ (10^6 rad s^{-1})	−3.80	−3.20 ± 0.04
B (10^{20} s^{-2})	5.7 ± 0.3	2.04 ± 0.06
τ_V^{310} (ps)[a]	24.6	21.2 ± 0.6

[a] $\tau_V^{310} = 0.985\tau_V^{298}$.

coordination sphere. Some parameters related to the electronic relaxation rate were fixed to usual values: the hyperfine coupling constant between the oxygen nucleus of the bound water molecule and the Gd^{III} ion ($A/\hbar = -3.8 \times 10^6$ rad s^{-1}),[46] the correlation time modulating the electronic relaxation of Gd^{III} ($\tau_V^{298} = 25$ ps),[46] and the activation energy related to τ_V ($E_V = 1$ kJ mol^{-1}).[47] This results in the determination of the following parameters: the residence time of the coordinated water molecules (τ_M); B, related to the mean-square of the zero-field-splitting energy Δ ($B = 2.4\Delta^2$); $\Delta H^{\ddagger}$ and $\Delta S^{\ddagger}$, respectively, the enthalpy and entropy of activation of the water exchange process. The calculated parameters are shown in Table 1.

The calculated value of the water residence time at 37 °C for $[\{Ru(bpy)_2\}_2Gd\{DTPA(ph\text{-}phen)_2\}(H_2O)]Cl_4$ is larger than that of Gd-DTPA (τ_M^{310} = 143 ns) because of the presence of two amide bonds but is smaller than that of Gd-DTPA-BMA (τ_M^{310} = 1050[46]−967 ns;[48] DTPA-BMA = 1,7-bis(methylcarbamoylmethyl)-1,4,7-triazaheptane-1,4,7-triacetic acid). The $[\{Ru(bpy)_2\}_2Gd\{DTPA(ph\text{-}phen)_2\}(H_2O)]Cl_4$ complex was investigated by proton nuclear magnetic relaxation dispersion (NMRD) measurements in water at 37 °C from 0.24×10^{-3} to 1.41 T, and the NMRD profile is shown in Figure 3. To exclude the possibility of stacking between the different molecules, the NMRD profile of $[\{Ru(bpy)_2\}_2Gd\{DTPA(ph\text{-}phen)_2\}(H_2O)]Cl_4$ was measured at two concentrations, 0.795 and 0.397 mM.

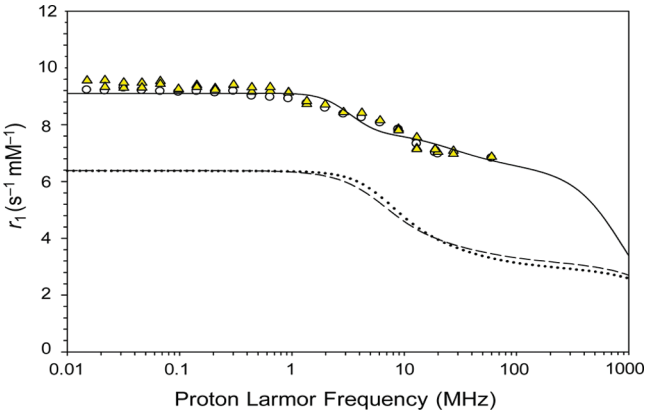

Figure 3. Proton relaxivity of $[\{Ru(bpy)_2\}_2Gd\{DTPA(ph\text{-}phen)_2\}(H_2O)]Cl_4$ at 37 °C; circles, [Gd] = 0.795 mM; triangles, [Gd] = 0.397 mM. The dotted line corresponds to the profile of Gd-DTPA and the dashed line to the profile of Gd-DTPA-BMA.

The theoretical fitting of the NMRD profiles takes into account the inner-[49,50] and outer[51]-sphere contributions to the paramagnetic relaxation rate. Some parameters were fixed during the fitting procedure: the distance (d) of closest approach for the outer-sphere contribution was set at 0.36 nm, τ_M was set to the value obtained by ^{17}O NMR (τ_M^{310} = 808 ns) as described above, the number of coordinated water molecules was set to 1 ($q = 1$), the relative diffusion constant $D = 3.0 \times 10^{-9}$ m^2 s^{-1}, and r is the distance between the Gd^{III} ion and the proton nuclei of water (r = 0.31 nm). The results of the fittings are shown in Figure 3 and Table 2. The NMRD profile of $[\{Ru(bpy)_2\}_2Gd\{DTPA(ph\text{-}phen)_2\}(H_2O)]Cl_4$ was fitted three times. When τ_V was fixed to the value used in ^{17}O NMR (τ_V = 24.6 ps), no good NMRD fitting was found according with the measured data. Therefore, the upper limit of τ_V was set free, resulting in a proper fitting but also a quite large value ($\tau_V = 50 \pm 3$ ps), so a third value (τ_V = 35 ps) was fixed to check if any notable changes were found. The agreement between these fitted results and the experimental data slightly changed, but the value of the electronic relaxation rate at very low field τ_{SO} [$\tau_{SO} = (5B\tau_V)^{-1}$] was not affected and the τ_R values changed by less than 12%. It is to be noted that the model used to fit the data assumes a spherical shape of the Gd^{III} complex. This assumption is probably not fulfilled for the $[\{Ru(bpy)_2\}_2Gd\{DTPA(ph\text{-}phen)_2\}(H_2O)]Cl_4$ complex.

At a frequency of 20 MHz, the NMRD profile of $[\{Ru(bpy)_2\}_2Gd\{DTPA(ph\text{-}phen)_2\}(H_2O)]Cl_4$ shows an increased proton relaxivity compared with Gd-DTPA and Gd-DTPA-BMA, which is the result of an increase of the rotational correlation time (τ_R) of $[\{Ru(bpy)_2\}_2Gd\{DTPA(ph\text{-}phen)_2\}(H_2O)]Cl_4$. The tumbling rate observed for $[\{Ru(bpy)_2\}_2Gd\{DTPA(ph\text{-}phen)_2\}(H_2O)]Cl_4$ decreases by a factor of about 4 compared to Gd-DTPA. This is in good agreement with the increase of the molecular weight of the complex. Finally, because contrast agents can show interaction with proteins, interaction studies with HSA were performed. HSA is one of the most important proteins in human plasma and has a constitution of 4−4.5% to plasma. MRI contrast agents can bind via a noncovalent interaction with HSA, reducing their mobility. Figure 4 displays the longitudinal proton relaxation rate in a solution containing 4% HSA, as a function of the $[\{Ru(bpy)_2\}_2Gd\{DTPA(ph\text{-}phen)_2\}(H_2O)]Cl_4$ concentration. The increase of the paramagnetic relaxation rate in the

Table 2. Parameters Obtained by the Theoretical Fitting of the Proton NMRD Data in Water at 310 K

parameter	$[\{Ru(bpy)_2\}_2Gd\{DTPA(ph\text{-}phen)_2\}(H_2O)]Cl_4$			Gd-DTPA-BMA[a]	Gd-DTPA[a]
τ_M^{310} (ns)	808[b]	808[b]	808[b]	967	143
τ_R^{310} (ps)	206 ± 5	223 ± 5	231 ± 4	65 ± 2	54 ± 14
τ_{SO}^{310} (ps)[d]	113 ± 2	112 ± 2	112 ± 1	95 ± 3	87 ± 3
τ_V^{310} (ps)	50 ± 3	35[c]	24.6[c]	18 ± 3	25 ± 3
r_1 (s^{-1} mM^{-1}) at 20 MHz	7.0	7.0	7.0	3.8	3.8

[a] From refs 48 and 52. [b] Fixed to the value obtained for τ_M^{310} by ^{17}O relaxometry. [c] Fixed value. [d] $\tau_{SO} = (5B\tau_V)^{-1}$.

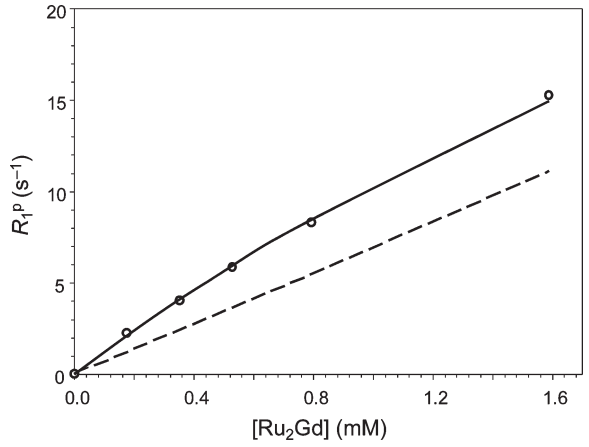

Figure 4. Proton paramagnetic relaxation rate of solutions of $[\{Ru(bpy)_2\}_2Gd\{DTPA(ph\text{-}phen)_2\}(H_2O)]Cl_4$ in water containing 4% HSA at 20 MHz and 37 °C. The dashed line represents the data obtained in the absence of HSA.

presence of HSA confirms a noncovalent interaction. When we fit these data by eq 1, an estimation of the association constant, K_a, and the relaxivity of the noncovalently bound complex, r_1^c, can be made.

$$R_1^{p,obs} = 1000\{(r_1^f s^0) + 0.5(r_1^c - r_1^f)[Np^0 + s^0 + K_a^{-1} - \sqrt{[(Np^0 + s^0 + K_a^{-1})^2 - 4Ns^0p^0]}]\} \quad (1)$$

In eq 1, p^0 is the protein concentration, s^0 is the concentration of the paramagnetic complex, and N is the number of independent and identical interaction sites. The data were fitted, resulting in the following parameters: a value of 7.2 ± 0.6 s^{-1} mM^{-1} for the relaxivity of the free contrast agent, a K_a value equal to 4500 ± 638 M^{-1}, and a r_1^c value of 14.3 ± 1.7 s^{-1} mM^{-1}. The number of equivalent and independent sites was set to 1.

The interaction between $[\{Ru(bpy)_2\}_2Gd\{DTPA(ph\text{-}phen)_2\}(H_2O)]Cl_4$ and HSA is also confirmed by ultrafiltration experiments.[53] The unbound $[\{Ru(bpy)_2\}_2Gd\{DTPA(ph\text{-}phen)_2\}(H_2O)]Cl_4$ fractions were separated from the bound fractions, and the bound $[\{Ru(bpy)_2\}_2Gd\{DTPA(ph\text{-}phen)_2\}(H_2O)]Cl_4$ concentration was calculated by subtracting the free $[\{Ru(bpy)_2\}_2Gd\{DTPA(ph\text{-}phen)_2\}(H_2O)]Cl_4$ concentration, measured by relaxometry, from the initial concentration. The total concentration of the Gd^{III} complex ranged from 0.20 to 0.78 mM, while the protein concentration was fixed at 4% (Figure S4 in the Supporting Information). Subsequently, the concentration of bound $[\{Ru(bpy)_2\}_2Gd\{DTPA(ph\text{-}phen)_2\}(H_2O)]Cl_4$ divided by its total concentration was plotted as a function of the total concentration. The results obtained by relaxometry and ultrafiltration are in very good agreement.

The NMRD profile of a solution of $[\{Ru(bpy)_2\}_2Gd\{DTPA(ph\text{-}phen)_2\}(H_2O)]Cl_4$ (0.79 mM) in 4% HSA is shown in Figure 5 (left). It is the sum of the diamagnetic relaxation rate of a 4% HSA solution, the paramagnetic relaxation rate of free $[\{Ru(bpy)_2\}_2Gd\{DTPA(ph\text{-}phen)_2\}(H_2O)]Cl_4$ and the paramagnetic relaxation rate of bound $[\{Ru(bpy)_2\}_2Gd\{DTPA(ph\text{-}phen)_2\}(H_2O)]Cl_4$. The free $[Gd]^f$ = 0.406 mM and complexed $[Gd]^c$ = 0.388 mM concentrations of the $[\{Ru(bpy)_2\}_2Gd\{DTPA(ph\text{-}phen)_2\}(H_2O)]Cl_4$ complex were calculated from the K_a value obtained above. The paramagnetic relaxation rate of free $[\{Ru(bpy)_2\}_2Gd\{DTPA(ph\text{-}phen)_2\}(H_2O)]Cl_4$ was obtained from its relaxivity in water and its concentration in the HSA solution. The NMRD profile of the Gd^{III} complex bound to HSA was then calculated by subtracting the diamagnetic relaxation rate and the paramagnetic relaxation rate of free $[\{Ru(bpy)_2\}_2Gd\{DTPA(ph\text{-}phen)_2\}(H_2O)]Cl_4$ from the observed relaxation rate and dividing the result by the concentration of bound $[\{Ru(bpy)_2\}_2Gd\{DTPA(ph\text{-}phen)_2\}(H_2O)]Cl_4$ (Figure 5, right). As expected, the profile shows a "hump" characteristic of slowly rotating paramagnetic species at higher magnetic fields. However, because of the slow water exchange rate, the relaxivity of the bound complex is quite low.

Photophysical Properties. *Ru^{II}-Centered Absorption and Luminescence.* The electronic absorption spectrum of $[\{Ru(bpy)_2\}_2Gd\{DTPA(ph\text{-}phen)_2\}(H_2O)]Cl_4$ displays bands due to spin-allowed d → π^* metal-to-ligand charge-transfer (^{1}MLCT) transitions at 456 nm and a shoulder at 425 nm (Figure 6 and Table S1 and Figure S5 in the Supporting Information). In addition, the intense band at 287 nm corresponds to the ligand-centered $\pi \rightarrow \pi^*$ transitions. The bands at 254 and 244 nm might be attributed to either $\pi \rightarrow \pi^*$ and/or d → π^* transitions, while the shoulder at 320 nm to Ru^{II}-centered d → d transitions. The excitation spectrum of the $[\{Ru(bpy)_2\}_2Gd\{DTPA(ph\text{-}phen)_2\}(H_2O)]Cl_4$ complex, recorded by monitoring the emission at 610 nm, resembles the absorption spectrum, displaying the bands at 285, 320sh, 425sh, and 455 nm (Figure 6, top). Upon excitation into the ^{1}MLCT band at 440 nm, the $[\{Ru(bpy)_2\}_2Gd\{DTPA(ph\text{-}phen)_2\}(H_2O)]Cl_4$ complex exhibits bright-red luminescence in the range 550−850 nm, centered at 620 nm, which is originating from the ^{3}MLCT excited states (Figure 6, bottom). The luminescence lifetime is 0.54 μs, which is 1.2-fold longer than that for the $[Ru(bpy)_2(phen)]$ complex with a nonderivatized 1,10-phenanthroline ligand.[54] The quantum yield of $[\{Ru(bpy)_2\}_2Gd\{DTPA(ph\text{-}phen)_2\}(H_2O)]Cl_4$ was determined using Rhodamine 101 as a standard and was found to be 4.7%. In general, the photophysical parameters of $[\{Ru(bpy)_2\}_2Gd\{DTPA(ph\text{-}phen)_2\}(H_2O)]Cl_4$ are comparable with those of other luminescent Ru^{II} complexes.[21−23]

dx.doi.org/10.1021/ic200726t |*Inorg. Chem.* 2011, 50, 10005–10014

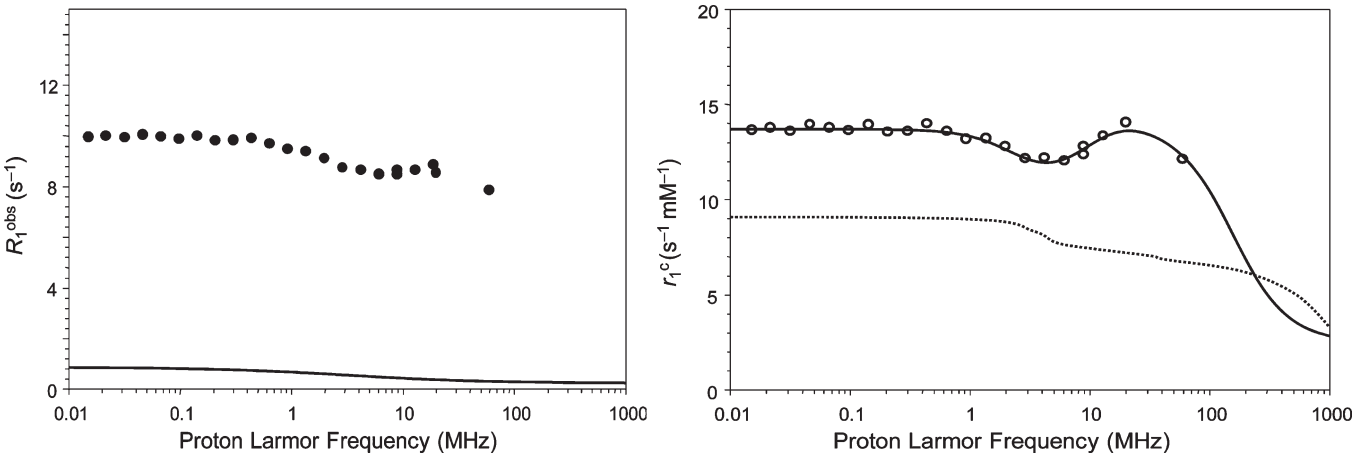

Figure 5. (Left) NMRD profile of $[\{Ru(bpy)_2\}_2Gd\{DTPA(ph\text{-}phen)_2\}(H_2O)]Cl_4$ (0.79 mM) in 4% HSA (closed circles) and that of 4% HSA (plain line). (Right) Calculated NMRD profile of $[\{Ru(bpy)_2\}_2Gd\{DTPA(ph\text{-}phen)_2\}(H_2O)]Cl_4$ bound to HSA (open circles). The line through the data is drawn to guide the eye. The relaxivity profile of $[\{Ru(bpy)_2\}_2Gd\{DTPA(ph\text{-}phen)_2\}(H_2O)]Cl_4$ in water is added for comparison (dotted line).

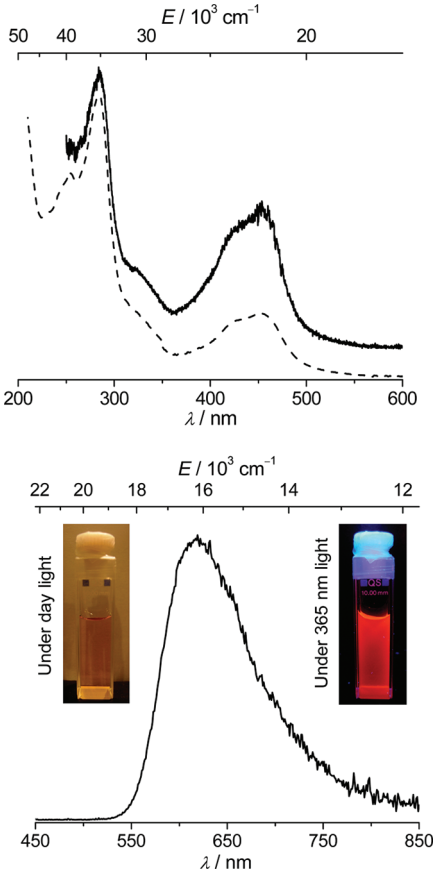

Figure 6. (Top) Excitation (λ_{em} = 610 nm, solid line), superimposed absorption (dashed line), and (bottom) emission (λ_{ex} = 440 nm) spectra, as well as photographs of a 10 μM aqueous solution of $[\{Ru(bpy)_2\}_2Gd\{DTPA(ph\text{-}phen)_2\}(H_2O)]Cl_4$.

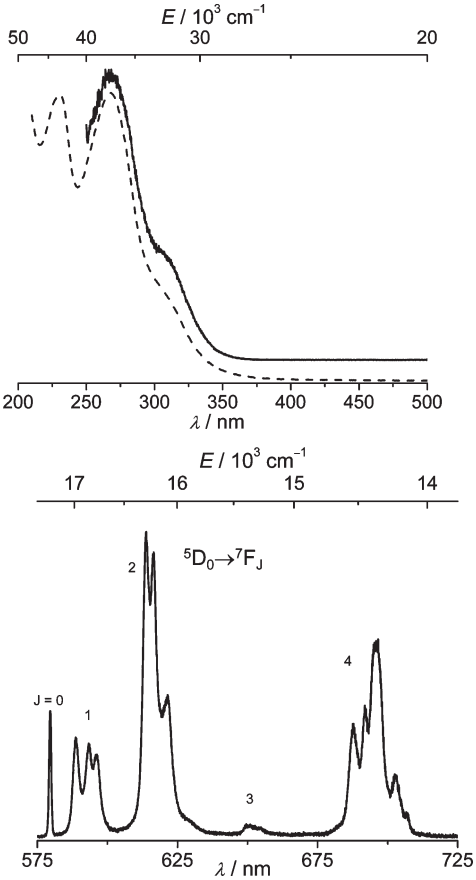

Figure 7. (Top) Excitation (λ_{em} = 614 nm, solid line), superimposed absorption (dashed line), and (bottom) emission (λ_{ex} = 300 nm) spectra of a 10 μM MeOH solution of $[Eu\{DTPA(ph\text{-}phen)_2\}(CH_3OH)]$.

$[\{Ru(bpy)_2\}_2Eu\{DTPA(ph\text{-}phen)_2\}(H_2O)]Cl_4$ displays absorption, excitation, and emission spectra very similar to those of its Gd^{III} analogue (Figures S5 and S6 in the Supporting Information). No characteristic Eu^{III} emission was observed under excitation into either the ^{1}MLCT or the $\pi\pi^*$ ligand band. This points to the existence of very efficient nonradiative deactivation quenching of Eu^{III} excited states.

Eu^{III}-Centered Luminescence. It is known that luminescent lanthanide ions can serve as probes of the coordination environment; moreover, solvation numbers can be determined by the

dx.doi.org/10.1021/ic200726t |*Inorg. Chem.* 2011, 50, 10005–10014

Table 4. Photophysical Parameters of the [Eu{DTPA-(ph-phen)$_2$}(CH$_3$OH)] Complex

solvent	τ_{obs}/ms[a]	τ_{rad}/ms[b]	Q_{Eu}^{Eu}[b]	Q_{Eu}^{L}[a]	η_{sens}/%[b]
MeOH	0.80(1)	4.35	18	0.77(7)	4.3(6)
MeOD	2.18(2)	4.42	49	2.3(2)	4.7(7)

[a] 2σ values within parentheses. [b] The refractive indexes for solutions taken as equal to these of neat solvents, n(MeOH) = 1.329 and n(MeOD) = 1.326; for the definition, see eqs 2 and 4.

lifetime method.[55,56] The nondegenerate $^5D_0$ emission state simplifies the interpretation of the luminescence spectra, so that the Eu^{III} ion is the most appropriate ion for use as a luminescent structural probe.

Because of the strong quenching of the f−f transitions by the MLCT states involving Ru^{II} in [{Ru(bpy)$_2$}$_2$Eu{DTPA-(ph-phen)$_2$}(H$_2$O)]Cl$_4$, the photophysical properties of [Eu{DTPA(ph-phen)$_2$}(CH$_3$OH)] in a MeOH solution have been investigated to gain insight into the coordination environment around the Ln ion offered by the DTPA(ph-phen)$_2$ ligand. [Eu{DTPA(ph-phen)$_2$}(CH$_3$OH)] exhibits ligand-centered absorption bands in the range 200−350 nm with maxima at 230 nm (ε = 56 805 M^{-1} cm^{-1}) and 268 nm (ε = 57 270 M^{-1} cm^{-1}) and a shoulder at 310 nm (ε = 16 370 M^{-1} cm^{-1}) (Figure 7, top). When the Eu^{III} $^5D_0 \rightarrow {}^7F_2$ transition at 614 nm is monitored, the excitation spectrum resembles the absorption spectrum. Upon excitation into the ligand levels, [Eu{DTPA(ph-phen)$_2$}-(CH$_3$OH)] exhibits characteristic bright-red luminescence due to the $^5D_0 \rightarrow {}^7F_J$ transitions (J = 0−4) (Figure 7, bottom; Table S2 in the Supporting Information). The hypersensitive $^5D_0 \rightarrow {}^7F_2$ transition is dominating the spectrum with $I(^5D_0 \rightarrow {}^5F_2)/I(^5D_0 \rightarrow {}^5F_1)$ = 2.9, while the $^5D_0 \rightarrow {}^7F_4$ transition also has a sizable intensity with $I(^5D_0 \rightarrow {}^5F_2)/I(^5D_0 \rightarrow {}^5F_1)$ = 2.5 (Table S3 in the Supporting Information). The highly forbidden $^5D_0 \rightarrow {}^7F_0$ transition has a quite large intensity (16% of the magnetic dipole $^5D_0 \rightarrow {}^7F_1$ transition), so the Eu^{III} ion is occupying a site with a C_s, C_n, or C_{nv} symmetry.

Quantitatively, the Eu^{III} luminescence can be analyzed using eq 2, where Q_{Eu}^{L} and Q_{Eu}^{Eu} are the overall and intrinsic quantum yields, η_{sens} is the sensitization efficiency, and τ_{obs} and τ_{rad} are the observed and radiative lifetimes of the Eu^{III} $^5D_0$ level:

$$Q_{Eu}^{L} = \eta_{sens} Q_{Eu}^{Eu} = \eta_{sens}\left(\frac{\tau_{obs}}{\tau_{rad}}\right) \quad (2)$$

The luminescence lifetimes of [Eu{DTPA(ph-phen)$_2$}-(CH$_3$OH)] in a MeOH solution (τ_{MeOH}) is equal to 0.80 ms, and it increases by 2.7 times when going to a deuterated MeOH (MeOD) solution (τ_{MeOD}), being in line with less nonradiative deactivation induced by O−D vibrations in comparison with O−H vibrations (Table 4). To estimate the number of solvent molecules coordinated to a Eu^{III} ion, Beeby's equation was used,[57] taking into account that an alcohol molecule has one O−H oscillator and thus causes twice less the effect than water:

$$q_{MeOH} = 2.4(\Delta k - 0.25 - 0.075q^{N}) \quad (3)$$

where $\Delta k = 1/\tau_{MeOH} - 1/\tau_{MeOD}$ and q^N is the number of coordinated amide groups. This resulted in q_{MeOH} = 0.9. So, the organic ligand in the [Eu{DTPA(ph-phen)$_2$}(CH$_3$OH)] complex arranges around the Eu^{III} ion in such a way that coordination of one solvent molecule is possible. Assuming that coordination of Ru^{II} to the 1,10-phenanthroline moieties will not significantly change the environment around the Ln^{III} ion, the solvation number of the lanthanide ions in the [{Ru(bpy)$_2$}$_2$Ln-{DTPA(ph-phen)$_2$}(H$_2$O)]Cl$_4$ complexes is considered to be 1.

The sensitized luminescence quantum yield of [Eu{DTPA-(ph-phen)$_2$}(CH$_3$OH)] in MeOH is 0.77%, and it increases up to 2.3% in MeOD being in agreement with the above discussion on nonradiative transitions. Because of the low absorption coefficients of f-f transitions of lanthanide ions the intrinsic quantum yield could not be measured and thus was estimated using eq 2 and the following relation for the radiative lifetime:

$$\frac{1}{\tau_{rad}} = A_{MD,0} \cdot n^3 \cdot \left(\frac{I_{tot}}{I_{MD}}\right) \quad (4)$$

where $A_{MD,0}$ is the Einstein coefficient and equals 14.65 s^{-1}, n is the refractive index, I_{tot} the total integrated intensity of $^5D_0 \rightarrow {}^7F_J$ (J = 0−4) and I_{MD} the integrated intensity of magnetic-dipole transition $^5D_0 \rightarrow {}^7F_1$. The values of 18 and 49% were obtained for [Eu{DTPA(ph-phen)$_2$}(CH$_3$OH)] in MeOH and MeOD (Table 4) following the same trend as τ_{obs} and Q_{Eu}^{L}. Although the Q_{Eu}^{Eu} value is reaching almost 50% for a MeOD solution, the overall luminescence quantum yield remains quite low as a result of the inefficient energy transfer from the organic ligand to the Eu^{III} ion. Indeed, the sensitization efficiency calculated as a ratio of quantum yields using eq 2 lies in the range 4.3−4.7%.

CONCLUSIONS

In this paper, the design of a new trinuclear heterobimetallic complex, [{Ru(bpy)$_2$}$_2$Ln{DTPA(ph-phen)$_2$}(H$_2$O)]Cl$_4$ (Ln = Eu, Gd), is presented. The formation of [{Ru(bpy)$_2$}$_2$Gd{DTPA-(ph-phen)$_2$}(H$_2$O)]Cl$_4$ results in a decrease of the tumbling rate by a factor of 3.8 in comparison with Gd-DTPA (Magnevist). ^{1}H NMRD measurements of [{Ru(bpy)$_2$}$_2$Gd{DTPA(ph-phen)$_2$}-(H$_2$O)]Cl$_4$ in water show a r_1 relaxivity at 20 MHz and 37 °C of 7.0 s^{-1} mM^{-1}. Furthermore, relaxometry and ultrafiltration experiments indicate that the DTPA(ph-phen)$_2$ ligand has a high affinity to noncovalently bind to HSA, resulting in a r_1 relaxivity of 14.3 s^{-1} mM^{-1} at 20 MHz and 37 °C. Unfortunately, the slow water exchange rate of [{Ru(bpy)$_2$}$_2$Gd{DTPA(ph-phen)$_2$}(H$_2$O)]Cl$_4$ restrains the increase of the longitudinal relaxation rate, resulting in a rather low relaxivity. [{Ru(bpy)$_2$}$_2$Gd{DTPA(ph-phen)$_2$}(H$_2$O)]-Cl$_4$ also shows interesting photophysical properties, exhibiting bright-red emission with a quantum yield of 4.7%. The luminescence lifetime of [{Ru(bpy)$_2$}$_2$Gd{DTPA(ph-phen)$_2$}(H$_2$O)]-Cl$_4$ is long enough to exceed any fluorescent background. Considering both the relaxometric and photophysical properties of [{Ru(bpy)$_2$}$_2$Gd{DTPA(ph-phen)$_2$}(H$_2$O)]Cl$_4$, it can act as a potential probe for time-gated luminescence-based imaging as well as a contrast agent for MRI.

EXPERIMENTAL SECTION

Materials. All reagents were obtained from Aldrich Chemical (Bornem, Belgium) and Acros Organics (Geel, Belgium) and were used without further purification. Europium(III) triflate was synthesized according to the literature procedure, starting from Eu$_2$O$_3$ (99.995%).[58]

Synthesis. *Synthesis of 5-Bromo-1,10-phenanthroline.* 5-Bromo-1,10-phenanthroline was prepared according to a literature procedure.[59]

Yield: 68%. Mp: 113 °C. ^{1}H NMR (300 MHz, CDCl$_3$, ppm): δ 9.20 (m, 2H), 8.66 (d, J = 7.8 Hz, 1H), 8.17 (dd, J = 1.8 and 8.2 Hz, 1H), 8.13 (s, 1 H), 7.74 (dd, J = 4.1 and 8.3 Hz, 1H), 7.65 (dd, J = 4.5 and 8.2 Hz, 1H). ^{13}C NMR (150 MHz, CDCl$_3$, ppm): δ 151.33, 151.10, 147.01,

146.03, 136.35, 135.52, 130.08, 129.20, 128.31, 124.23, 124.07, 121.22. HRMS (EI). Calcd for $C_{12}H_7BrN_2$ [M]: m/z 257.9793. Found: m/z 257.9792.

*Synthesis of tert-Butyl [4-(1,10-Phenanthrolin-5-yl)phenyl]carbamate (**1**).* To a solution of 5-bromo-1,10-phenanthroline (399 mg, 1.54 mmol), *tert*-butyl [4-(4,4,5,5-tetramethyl-1,3,2-dioxaborolan-2-yl)phenyl]carbamate (538 mg, 1.69 mmol, 1.1 equiv), and Cs_2CO_3 (1.01 g, 3.10 mmol, 2 equiv) in a 1:1 H_2O/toluene biphasic mixture (32 mL) was added 10 mol % of $Pd(PPh_3)_4$ (178 mg), and the resulting solution was refluxed for 16 h. The reaction mixture was added to CH_2Cl_2 (100 mL) and water (100 mL) and thoroughly stirred, and the organic layer was separated. The aqueous layer was extracted twice with CH_2Cl_2 (100 mL), the combined organic layer was dried over Na_2SO_4 and evaporated in vacuo, and the residue was purified by column chromatography [silica gel, CH_2Cl_2 (saturated NH_3)]. After evaporation, the product was recrystallized from hot toluene (25 mL) and collected as a white solid (387 mg, 68%).

Mp: >250 °C, product starts to decompose at 258 °C. ^{1}H NMR (300 MHz, $CDCl_3$, ppm): δ 9.20 (s, 2H), 8.30 (dd, J = 1.4 and 8.2 Hz, 1H), 8.24 (d, J = 8.3 Hz, 1H), 7.71 (s, 1H), 7.65 (dd, J = 4.5 and 8.1 Hz, 1H), 7.60−7.55 (m, 3H), 7.46 (d, J = 8.3, 2H), 6.71 (s, 1H), 1.56 (s, 9H). ^{13}C NMR (150 MHz, $CDCl_3$, ppm): δ 153.19, 150.61, 150.45, 146.85, 146.14, 138.82, 138.73, 136.32, 134.96, 133.82, 130.99, 129.45, 128.63, 126.76, 123.74, 123.19, 119.01, 81.29, 28.75. HRMS (EI). Calcd for $C_{23}H_{21}N_3O_2$ [M]: m/z 371.1634. Found: m/z 371.1632.

*Synthesis of 4-(1,10-Phenanthrolin-5-yl)aniline (**2**).* To a solution of *tert*-butyl [4-(1,10-phenanthrolin-5-yl)phenyl]carbamate (387 mg, 1.04 mmol) in CH_2Cl_2 (10 mL) was added TFA (10 mL) dropwise, and the solution was stirred overnight at room temperature. The solvent was removed in vacuo, and the residue was purified by column chromatography [silica gel, CH_2Cl_2 (saturated NH_3)] and collected as a yellow solid (229 mg, 81%).

Mp: >250 °C, product starts to decompose at 258 °C. ^{1}H NMR (300 MHz, $CDCl_3$, ppm): δ 9.18 (m, 2H), 8.37 (d, J = 8.3 Hz, 1H), 8.21 (d, J = 8.3 Hz, 1H), 7.69 (s, 1H), 7.62 (dd, J = 8.3 and 4.6 Hz, 1H), 7.57 (dd, J = 8.3 and 4.6 Hz, 1H), 7.32 (d, J = 8.4 Hz, 2H), 6.84 (d, J = 8.4 Hz, 2H), 3.87 (br s, 2H). ^{13}C NMR (150 MHz, $CDCl_3$, ppm): δ 150.29, 146.89, 146.76, 145.95, 139.40, 136.19, 135.13, 131.35, 129.19, 128.66, 126.39, 123.65, 123.07, 115.41. HRMS (EI). Calcd for $C_{18}H_{13}N_3$ [M]: m/z 271.1109. Found: m/z 271.1110.

Synthesis of Bis(1,10-phenanthroline) Derivative [DTPA(ph-phen)$_2$]. A mixture of 4-(1,10-phenanthrolin-5-yl)aniline (100 mg, 0.36 mmol, 2 equiv) and diethylenetriaminepentaacetic acid bisanhydride (64 mg, 0.18 mmol, 1 equiv) in DMF (7 mL) was stirred overnight at 60 °C. Diethyl ether (100 mL) was added to the reaction mixture at 0 °C, and DTPA(ph-phen)$_2$ (148 mg, 89%) was collected as a precipitate and used without further purification. IR spectral data show strong absorption at 1661 cm^{-1} due to the C═O stretching mode of the free acid. The lower energy of the C═O vibrations can be explained by intramolecular hydrogen bonding.

Mp: 189 °C. ^{1}H NMR (400 MHz, DMSO-d_6, ppm): δ 9.12 (d, J = 4.5 Hz, 2H), 9.02 (d, J = 4.2 Hz, 2 H), 8.41 (d, J = 8.4 Hz, 2H), 8.33 (d, J = 8.5 Hz, 2H), 7.89 (dd, J = 8.4 and 4.5 Hz, 2H), 7.79 (d, J = 8.2 Hz, 4H), 7.72 (dd, J = 8.5 and 4.2 Hz, 2H), 7.58 (s, 2H), 7.27 (d, J = 8.2 Hz, 4H), 4.20 (s, 2H), 4.08 (s, 4H), 3.87−3.81 (m, 8H), 3.63 (t, J = 6.1 Hz, 4H). ^{13}C NMR (100 MHz, DMSO-d_6, ppm): δ 173.58, 170.10, 150.31, 150.06, 146.19, 145.31, 139.10, 138.18, 136.57, 134.46, 133.52, 130.58, 128.29, 127.67, 126, 87, 123.98, 123.58, 119.91, 58.94, 55.90, 52.91, 51.58. IR (KBr): 1661 (CO free acid), 1603 (amide I), 1519 (amide II) cm^{-1}. ESI-MS. Calcd for $C_{50}H_{45}N_9O_8$ [M − H]$^-$: m/z 898.9. Found: m/z 898.3.

Synthesis of Ln^{III} Complexes. To a solution of DTPA(ph-phen)$_2$ (50 mg, 0.06 mmol, 1 equiv) in MeOH (5 mL) was added the corresponding lanthanide(III) triflate (0.06 mmol, 1 equiv), and the mixture was stirred at 50 °C for 24 h under an argon atmosphere. The solution was concentrated under reduced pressure, redissolved in a small amount of MeOH, and precipitated by diethyl ether. The purity was checked by HPLC with MeOH/H_2O and 0.1% TFA as eluents, resulting in a single peak. Free Ln ions were removed by Chelex 100, and their absence was checked by a test with an arsenazo indicator solution. A shift of approximately 65 cm^{-1} to lower energy is observed for the carbonyl stretching in IR spectra of [Ln{DTPA(ph-phen)$_2$}(CH$_3$OH)], thus confirming complexation of the Ln ion by the ligand.

Eu^{III} complex [Eu{DTPA(ph-phen)$_2$}(CH$_3$OH)]. Yield: 45.7 mg (78%). IR (KBr): 1595 (COO^- asym stretch), 1544 (amide II), 1400 (COO^- sym stretch) cm^{-1}. ESI-MS. Calcd for $C_{50}H_{42}EuN_9O_8$: m/z 1072.2 ([M + Na]$^+$), 547.4 ([M + 2Na]$^{2+}$). Found: m/z 1072.9 ([M + Na]$^+$), 548.3 ([M + 2Na]$^{2+}$). HPLC (solvent A, H_2O + 0.1% HCOOH; solvent B, MeOH, 20% B → 100% B, 20 min): t_r 20.65 min.

Gd^{III} complex [Gd{DTPA(ph-phen)$_2$}(CH$_3$OH)]. Yield: 45.2 mg (77%). IR (KBr): 1598 (COO^- asym stretch), 1548 (amide II), 1400 (COO^- sym stretch) cm^{-1}. ESI-MS. Calcd for ($C_{50}H_{42}GdN_9O_8$ [M]: m/z 528.1 ([M + 2H]$^{2+}$), 352.3 ([M + 3H]$^{3+}$). Found: m/z 527.9 ([M + 2H]$^{2+}$), 352.2 ([M + 3H]$^{3+}$). HPLC (solvent A, H_2O + 0.1% HCOOH; solvent B, MeOH, 20% B → 100% B, 20 min): t_r 20.27 min.

Synthesis of Ln^{III}−Ru^{II} Complexes. cis-[$RuCl_2$(bpy)$_2$] was synthesized following a literature procedure.[60]

A solution of *cis*-[$RuCl_2$(bpy)$_2$] (17.2 mg, 0.036 mmol, 2 equiv) in a 1:1 H_2O/EtOH mixture (2 mL) was refluxed under an argon atmosphere for 5 h, the corresponding [Ln{DTPA(ph-phen)$_2$}(CH$_3$OH)] complex was added (20 mg, 0.02 mmol, 1 equiv), and the mixture was refluxed overnight. The solution was concentrated under reduced pressure at 50 °C, and the resulting dark-violet product was purified by HPLC. The collected fractions were concentrated under reduced pressure and dried overnight under vacuum at 50 °C. The purity of the compound was checked again by HPLC with ACN/H_2O and 0.1% TFA as eluents, resulting in a single peak. The HPLC analysis of [{Ru(bpy)$_2$}$_2$Gd{DTPA(ph-phen)$_2$}(H_2O)]Cl_4 is shown in the Supporting Information (Figure S3).

Eu^{III} complex [{Ru(bpy)$_2$}$_2$Eu{DTPA(ph-phen)$_2$}(H_2O)]Cl_4. Yield: 59%. IR (KBr): 1596 (COO^- asym stretch), 1544 (amide II), 1417 (COO^- sym stretch) cm^{-1}. ESI-MS. Calcd for $C_{90}H_{74}EuN_{17}O_8Ru_2$ [M]: m/z 643.1 ([M + H_2O + Cl]$^{3+}$), 482.4 ([M + 3H_2O]$^{4+}$), 386.2 ([M + H + 3H_2O]$^{5+}$), 240.5 ([M + 2H + 2Na]$^{8+}$). Found: m/z 644.0 ([M + H_2O + Cl]$^{3+}$), 483.2 ([M + 3H_2O]$^{4+}$), 386.8 ([M + H + 3H_2O]$^{5+}$), 240.1 ([M + 2H + 2Na]$^{8+}$). HPLC (solvent A, H_2O + 0.1% HCOOH; solvent B, ACN, 10% B → 50% B, 30 min): t_r 17.24 min.

Gd^{III} complex [{Ru(bpy)$_2$}$_2$Gd{DTPA(ph-phen)$_2$}(H_2O)]Cl_4. Yield: 36%. IR (KBr): 1598 (COO^- asym stretch), 1548 (amide II), 1419 (COO^- sym stretch) cm^{-1}. ESI-MS. Calcd for $C_{90}H_{74}GdN_{17}O_8Ru_2$ [M]: m/z 644.8 ([M + H_2O + Cl]$^{3+}$), 483.7 ([M + 3H_2O]$^{4+}$), 387.2 ([M + H + 3H_2O]$^{5+}$), 241.1 ([M + 2H + 2Na]$^{8+}$). Found: m/z 644.2 ([M + H_2O + Cl]$^{3+}$), 483.3 ([M + 3H_2O]$^{4+}$), 386.7 ([M + H + 3H_2O]$^{5+}$), 240.1 ([M + 2H + 2Na]$^{8+}$). HPLC (solvent A, H_2O + 0.1% HCOOH; solvent B, ACN, 10% B → 50% B, 30 min): t_r 15.81 min.

Instruments. ^{1}H and ^{13}C NMR spectra were recorded by using a Bruker Avance 300 spectrometer (Bruker, Karlsruhe, Germany), operating at 300 MHz for ^{1}H and 75 MHz for ^{13}C, a Bruker Avance 400 spectrometer, operating at 400 MHz for ^{1}H and 100 MHz for ^{13}C, and a Bruker Avance 600 spectrometer operating at 150 MHz for ^{13}C. IR spectra were measured by using a Bruker Alpha-T FT-IR spectrometer (Bruker, Ettlingen, Germany), and data were processed with *OPUS 6.5* software. The LC/MS data were collected using an Agilent 1100 system coupled to an Agilent 6110 single-quadrupole MS system. The LC/MS method used a Grace Prevail RP-C_{18} column (150 mm × 2.1 mm; particle size 3 μm). ESI-MS spectra were obtained by using a Thermo Finnigan LCQ Advantage mass spectrometer. Preparative HPLC was performed using a Waters Delta 600 system equipped with a Waters 996 photodiode-array detector. The preparative HPLC method used a

Phenomenex Luna C_{18} column (150 mm × 21.20 mm; particle size 5 μm). Melting points were determined using a Reichert-Jung Thermovar apparatus and were uncorrected.

Photophysical Measurements. All photophysical measurements were performed on 10 μM solutions in degassed solvents. Absorption spectra were recorded with a Varian Cary 5000 spectrophotometer using quartz Suprasil cells (115F-QS; path length 0.2 cm). Excitation and luminescence spectra were recorded on Edinburgh Instruments FS900 or FS920 steady-state spectrofluorimeters using the same cells and measuring the emitted light at the right angle and along the long (1 cm) path length. The spectrofluorimeters are equipped with a 450 W xenon arc lamp, a microsecond flashlamp (pulse length 2 μs), and a red-sensitive (300−850 nm, Hamamatsu R928P on FS920) or an extended red-sensitive (185−1010 nm, Hamamatsu R2658P on FS920) photomultiplier. All spectra were corrected for the instrumental functions. Luminescence lifetimes of the $^5D_0$ level for Eu^{III}-containing solutions were measured on an Edinburgh Instruments FS920 steady-state spectrofluorimeter under 280−300 nm excitation. Lifetimes are averages of at least three independent measurements. Quantum yields were determined by a comparative method using Rhodamine 101 (Aldrich) in ethanol (Q = 100%) as a standard.[61] Luminescence lifetimes of Ru^{II} emission in $[\{Ru(bpy)_2\}_2Gd\{DTPA(ph\text{-}phen)_2\}(H_2O)]Cl_4$ under excitation into the MLCT band were determined using the time-correlated single-photon-counting technique described in detail previously.[62] All measurements were performed at room temperature.

Framework Molecular Model. The model was built using the *Avogadro* software package. The geometry of the Gd^{III}−Ru^{II} complex was optimized with the universal force field.[63]

^{17}O NMR. ^{17}O NMR measurements of solutions were performed on 350 μL samples placed in 5-mm-external-diameter tubes on a Bruker Avance-500 spectrometer (Bruker, Karlsruhe, Germany). The temperature was regulated by air or nitrogen-flow-controlled by a Bruker BVT 3200 unit. ^{17}O transverse relaxation times of distilled water (pH = 6.5−7) were measured using a CPMG sequence and a subsequent two-parameter fit of the data points. The 90° and 180° pulse lengths were 27.5 and 55 μs, respectively. ^{17}O T_2 of water in a complex solution was obtained from line-width measurements. All spectra were proton-decoupled. The concentration of $[\{Ru(bpy)_2\}_2Gd\{DTPA(ph\text{-}phen)_2\}(H_2O)]Cl_4$ was equal to 6.81 mM. The data are presented as the reduced transverse relaxation rate ($1/T_2^R = 55.55/T_2^{para}[Gd]$, where [Gd] is the molar concentration of the complexed Gd^{III}, q is the number of coordinated water molecules, and T_2^{para} is the paramagnetic transverse relaxation rate). The treatment of the experimental data was performed as described previously.[42,43]

Proton NMRD. Proton NMRD profiles were measured on a Stelar Spinmaster FFC, fast-field-cycling NMR relaxometer (Stelar, Mede (PV), Italy) over a magnetic field strength range extending from 0.24 mT to 1.4 T. Measurements were performed on 0.6 mL samples contained in 10-mm-o.d. Pyrex tubes. Additional relaxation rates at 20 and 60 MHz were respectively obtained on a Minispec mq20 and a Minispec mq60 (Bruker, Karlsruhe, Germany). The proton NMRD curves were fitted using data-processing software,[64] including different theoretical models describing the nuclear relaxation phenomena (Minuit, CERN Library).[49−51]

Proton Relaxometry in a HSA Solution. The interaction with HSA was studied by proton relaxometry at 20 MHz and 37 °C on a Bruker Minispec mq20. The concentration of HSA was kept constant (4%), and the concentration of $[\{Ru(bpy)_2\}_2Gd\{DTPA(ph\text{-}phen)_2\}(H_2O)]Cl_4$ was varied.

Ultrafiltration Experiment with HSA. During the ultrafiltration measurement in HSA solutions, the unbound ligand fraction was separated by centrifugation using the Amicon Ultra centrifugal filter and a Ultracell-10K tube (Millipore). The free ligand concentration was obtained by proton relaxometry (three to five T_1 measurements). The bound ligand concentration was calculated by subtracting the free ligand concentration measured by relaxometry from the initial concentration. The relative error on the T_1 measurements was 3%.

■ ASSOCIATED CONTENT

Supporting Information. ^{1}H and 2D COSY NMR spectra of ligand $DTPA(ph\text{-}phen)_2$ in DMSO-d_6 (Figures S1 and S2), HPLC analysis of $[\{Ru(bpy)_2\}_2Gd\{DTPA(ph\text{-}phen)_2\}(H_2O)]Cl_4$ (Figure S3), ultrafiltration and relaxometry results of $[\{Ru(bpy)_2\}_2Gd\{DTPA(ph\text{-}phen)_2\}(H_2O)]Cl_4$ (Figure S4), absorption spectra of $[\{Ru(bpy)_2\}_2Ln\{DTPA(ph\text{-}phen)_2\}(H_2O)]Cl_4$ (Figures S5 and S6), excitation and emission spectra of $[\{Ru(bpy)_2\}_2Eu\{DTPA(ph\text{-}phen)_2\}(H_2O)]Cl_4$ (Figure S7), mass spectra of all synthesized compounds (Figures S8−S15), as well as (i) the assignment of the bands in the absorption spectrum of $[\{Ru(bpy)_2\}_2Gd\{DTPA(ph\text{-}phen)_2\}(H_2O)]Cl_4$ (Table S1), (ii) the main peaks in the emission spectrum of $[Eu\{DTPA(ph\text{-}phen)_2\}(CH_3OH)]$ (Table S2), and (iii) relative integral intensities of f−f transitions for $[Eu\{DTPA(ph\text{-}phen)_2\}(CH_3OH)]$ (Table S3). This material is available free of charge via the Internet at http://pubs.acs.org.

■ AUTHOR INFORMATION

Corresponding Author

*E-mail: tatjana.vogt@chem.kuleuven.be.

■ ACKNOWLEDGMENT

G.D. and P.V. acknowledge the IWT Flanders (Belgium) for financial support. T.N.P.-V. and K.B. thank the FWO-Flanders (for Projects G.0412.09 and KAN2008 1.5.157.08). S.V.E. is a visiting postdoctoral fellow of the FWO-Flanders (Project G.0412.09). S.L., L.V.E., and R.N.M. thank the FNRS, the ARC program (Contract 05/10 335), the ENCITE program, and the EMIL program, the Interuniversity Attraction Poles P6/29 of the Belgian Federal Science Policy Office, and the COST Action D38. CHN microanalysis was performed by Dirk Henot. ESI-MS measurements were made by Dirk Henot and Bert Demarsin, and inductively coupled plasma mass spectrometry measurements were performed by Michèle Vanroelen (Department of Chemical Engineering). Karel Duerinckx is acknowledged for his help in the NMR measurements and Dr. Lesley Pandey for lifetime determination on $\{Gd[Ru(bpy)_2]_2DTPA(ph\text{-}phen)_2\}^{4+}$. We also thank Servaas Michielssens for his development of the framework molecular model.

■ REFERENCES

(1) Bonnet, C. S.; Toth, E. *C. R. Chim.* **2010**, *13*, 700.
(2) Frullano, L.; Meade, T. J. *J. Biol. Inorg. Chem.* **2007**, *12*, 939.
(3) Louie, A. *Chem. Rev.* **2010**, *110*, 3146.
(4) Bernhard, C.; Goze, C.; Rousselin, Y.; Denat, F. *Chem. Commun.* **2010**, *46*, 8267.
(5) Aime, S.; Barge, A.; Cabella, C.; Crich, S. G.; Gianolio, E. *Curr. Pharm. Biotechnol.* **2004**, *5*, 509.
(6) Beeby, A.; Botchway, S. W.; Clarkson, I. M.; Faulkner, S.; Parker, A. W.; Parker, D.; Williams, J. A. G. *J. Photochem. Photobiol. B* **2000**, *57*, 83.
(7) Charbonniere, L. J.; Ziessel, R.; Montalti, M.; Prodi, L.; Zaccheroni, N.; Boehme, C.; Wipff, G. *J. Am. Chem. Soc.* **2002**, *124*, 7779.
(8) Koullourou, T.; Natrajan, L. S.; Bhavsar, H.; Pope, S. J. A.; Feng, J. H.; Narvainen, J.; Shaw, R.; Scales, E.; Kauppinen, R.; Kenwright, A. M.; Faulkner, S. *J. Am. Chem. Soc.* **2008**, *130*, 2178.
(9) Weissleder, R.; Ntziachristos, V. *Nat. Med.* **2003**, *9*, 123.

(10) Bünzli, J.-C. G. *Chem. Rev.* **2010**, *110*, 2729.
(11) Gahlaut, N.; Miller, L. W. *Cytometry, Part A* **2010**, *77A*, 1113.
(12) Fernandez-Moreira, V.; Thorp-Greenwood, F. L.; Coogan, M. P. *Dalton Trans.* **2010**, *46*, 186.
(13) Manning, H. C.; Goebel, T.; Thompson, R. C.; Price, R. R.; Lee, H.; Bornhop, D. J. *Bioconjugate Chem.* **2004**, *15*, 1488.
(14) Crich, S. G.; Biancone, L.; Cantaluppi, V.; Esposito, D. D. G.; Russo, S.; Camussi, G.; Aime, S. *Magn. Reson. Med.* **2004**, *51*, 938.
(15) Kotkova, Z.; Kotek, J.; Jirak, D.; Jendelova, P.; Herynek, V.; Berkova, Z.; Hermann, P.; Lukes, I. *Chem.—Eur. J.* **2010**, *16*, 10094.
(16) Huber, M. M.; Staubli, A. B.; Kustedjo, K.; Gray, M. H. B.; Shih, J.; Fraser, S. E.; Jacobs, R. E.; Meade, T. J. *Bioconjugate Chem.* **1998**, *9*, 242.
(17) Moriggi, L.; Aebischer, A.; Cannizzo, C.; Sour, A.; Borel, A.; Bünzli, J.-C. G.; Helm, L. *Dalton Trans.* **2009**, 2088.
(18) Howes, P.; Green, M.; Bowers, A.; Parker, D.; Varma, G.; Kallumadil, M.; Hughes, M.; Warley, A.; Brain, A.; Botnar, R. *J. Am. Chem. Soc.* **2010**, *132*, 9833.
(19) Cai, B.; Yang, P.; Dai, J. W.; Wu, J. Z. *Cryst. Eng. Comm.* **2011**, *13*, 985.
(20) Jin, T.; Yoshioka, Y.; Fujii, F.; Komai, Y.; Seki, J.; Seiyama, A. *Chem. Commun.* **2008**, 5764.
(21) Kalyanasundaram, K. *Coord. Chem. Rev.* **1982**, *46*, 159.
(22) Juris, A.; Balzani, V.; Barigelletti, F.; Campagna, S.; Belser, P.; von Zelewsky, A. *Coord. Chem. Rev.* **1988**, *84*, 85.
(23) Campagna, S.; Puntoriero, F.; Nastasi, F.; Bergamini, G.; Balzani, V. In *Photochemistry and Photophysics of Coordination Compounds I*; Balzani, V., Campagna, S., Eds.; Springer: Berlin/Heidelberg, 2007; pp 117−214.
(24) Lo, K. K. W.; Lee, T. K. M.; Lau, J. S. Y.; Poon, W. L.; Cheng, S. H. *Inorg. Chem.* **2008**, *47*, 200.
(25) Anderson, A. J.; Jayanetti, S.; Mayanovic, R. A.; Bassett, W. A.; Chou, I. M. *Am. Mineral.* **2002**, *87*, 262.
(26) Lazarides, T.; Sykes, D.; Faulkner, S.; Barbieri, A.; Ward, M. D. *Chem.—Eur. J.* **2008**, *14*, 9389.
(27) Baca, S. G.; Adams, H.; Sykes, D.; Faulkner, S.; Ward, M. D. *Dalton Trans.* **2007**, 2419.
(28) Senechal-David, K.; Pope, S. J. A.; Quinn, S.; Faulkner, S.; Gunnlaugsson, T. *Inorg. Chem.* **2006**, *45*, 10040.
(29) Vazquez Lopez, M.; Eliseeva, S. V.; Blanco, J. M.; Rama, G.; Bermejo, M. R.; Vazquez, M. E.; Bünzli, J.-C. G. *Eur. J. Inorg. Chem.* **2010**, *2010*, 4532.
(30) Nonat, A. M.; Allain, C.; Faulkner, S.; Gunnlaugsson, T. *Inorg. Chem.* **2010**, *49*, 8449.
(31) Ji, J.; Rosenzweig, N.; Jones, I.; Rosenzweig, Z. *J. Biomed. Opt.* **2002**, *7*, 404.
(32) Erkkila, K. E.; Odom, D. T.; Barton, J. K. *Chem. Rev.* **1999**, *99*, 2777.
(33) Dobrucki, J. W. *J. Photochem. Photobiol. B* **2001**, *65*, 136.
(34) Barton, J. K.; Danishefsky, A. T.; Goldberg, J. M. *J. Am. Chem. Soc.* **1984**, *106*, 2172.
(35) Schmitt, F.; Govindaswamy, P.; Zava, O.; Suss-Fink, G.; Juillerat-Jeanneret, L.; Therrien, B. *J. Biol. Inorg. Chem.* **2009**, *14*, 101.
(36) Schmitt, F.; Govindaswamy, P.; Suss-Fink, G.; Ang, W. H.; Dyson, P. J.; Juillerat-Jeanneret, L.; Therrien, B. *J. Med. Chem.* **2008**, *51*, 1811.
(37) Scolaro, C.; Chaplin, A. B.; Hartinger, C. G.; Bergamo, A.; Cocchietto, M.; Keppler, B. K.; Sava, G.; Dyson, P. J. *Dalton Trans.* **2007**, 5065.
(38) Auzias, M.; Therrien, B.; Suss-Fink, G.; Stepnicka, P.; Ang, W. H.; Dyson, P. J. *Inorg. Chem.* **2008**, *47*, 578.
(39) Livramento, J. B.; Sour, A.; Borel, A.; Merbach, A. E.; Toth, V. *Chem.—Eur. J.* **2006**, *12*, 989.
(40) Livramento, J. B.; Toth, E.; Sour, A.; Borel, A.; Merbach, A. E.; Ruloff, R. *Angew. Chem., Int. Ed.* **2005**, *44*, 1480.
(41) Onishi, H.; Sekine, K. *Talanta* **1972**, *19*, 473.
(42) Muller, R. N.; Raduchel, B.; Laurent, S.; Platzek, J.; Pierart, C.; Mareski, P.; Vander Elst, L. *Eur. J. Inorg. Chem.* **1999**, 1949.
(43) Laurent, S.; Houze, S.; Vander Elst, L.; Guerit, N.; Muller, R. N. *Helv. Chim. Acta* **2000**, *83*, 394.
(44) Botteman, F.; Nicolle, G. M.; Vander Elst, L.; Laurent, S.; Merbach, A. E.; Muller, R. N. *Eur. J. Inorg. Chem.* **2002**, 2686.
(45) Micskei, K.; Powell, D. H.; Helm, L.; Brucher, E.; Merbach, A. E. *Magn. Reson. Chem.* **1993**, *31*, 1011.
(46) Powell, D. H.; Dhubhghaill, O. M. N.; Pubanz, D.; Helm, L.; Lebedev, Y. S.; Schlaepfer, W.; Merbach, A. E. *J. Am. Chem. Soc.* **1996**, *118*, 9333.
(47) Rudovsky, J.; Kotek, J.; Hermann, P.; Lukes, I.; Mainero, V.; Aime, S. *Org. Biomol. Chem.* **2005**, *3*, 112.
(48) Laurent, S.; Vander Elst, L.; Muller, R. N. *Contrast Media Mol. Imaging* **2006**, *1*, 128.
(49) Solomon, I. *Phys. Rev.* **1955**, *99*, 559.
(50) Bloembergen, N. *J. Chem. Phys.* **1957**, *27*, 572.
(51) Freed, J. H. *J. Chem. Phys.* **1978**, *68*, 4034.
(52) Laurent, S.; Vander Elst, L.; Botteman, F.; Muller, R. N. *Eur. J. Inorg. Chem.* **2008**, 4369.
(53) Henrotte, V.; Vander Elst, L.; Laurent, S.; Muller, R. *J. Biol. Inorg. Chem.* **2007**, *12*, 929.
(54) Ji, S.; Wu, W.; Wu, W.; Song, P.; Han, K.; Wang, Z.; Liu, S.; Guo, H.; Zhao, J. *J. Mater. Chem.* **2010**, *20*, 1953.
(55) Bünzli, J.-C. G. In *Lanthanide Probes in Life, Chemical and Earth Sciences. Theory and Practice*; Bünzli, J.-C. G., Choppin, G. R., Eds.; Elsevier Science Publishers BV: Amsterdam, The Netherlands, 1989; Chapter 7; pp 219−293.
(56) Bünzli, J.-C. G.; Eliseeva, S. V. In *Springer Series on Fluorescence. Lanthanide Luminescence: Photophysical, Analytical and Biological Aspects*; Hanninen, P., Harma, H., Eds.; Springer Verlag: Berlin, 2011; Vol. 7; pp 1−45.
(57) Beeby, A.; Clarkson, I. M.; Dickins, R. S.; Faulkner, S.; Parker, D.; Royle, L.; de Sousa, A. S.; Williams, J. A. G.; Woods, M. *J. Chem. Soc., Perkin Trans. 2* **1999**, 493.
(58) Goossens, K.; Nockemann, P.; Driesen, K.; Goderis, B.; Goerller-Walrand, C.; Van Hecke, K.; Van Meervelt, L.; Pouzet, E.; Binnemans, K.; Cardinaels, T. *Chem. Mater.* **2008**, *20*, 157.
(59) Girardot, C.; Lemercier, G.; Mulatier, J.-C.; Chauvin, J.; Baldeck, P. L.; Andraud, C. *Dalton Trans.* **2007**, 3421.
(60) Cardinaels, T.; Ramaekers, J.; Driesen, K.; Nockemann, P.; Van Hecke, K.; Van Meervelt, L.; Goderis, B.; Binnemans, K. *Inorg. Chem.* **2009**, *48*, 2490.
(61) Eaton, D. F. *Pure Appl. Chem.* **1988**, *60*, 1107.
(62) Maus, M.; Rousseau, E.; Cotlet, M.; Schweitzer, G.; Hofkens, J.; Van der Auweraer, M.; De Schryver, F. C.; Krueger, A. *Rev. Sci. Instrum.* **2001**, *72*, 36.
(63) Rappe, A. K.; Casewit, C. J.; Colwell, K. S.; Goddard, W. A.; Skiff, W. M. *J. Am. Chem. Soc.* **1992**, *114*, 10024.
(64) Muller, R. N.; Declercq, D.; Vallet, P.; Giberto, F.; Daminet, B.; Fischer, H. W.; Maton, F.; Van Haverbeke, Y. *Proceedings of ESMRMB 7th Annual Congress*, Strasbourg, France, 1990; Vol. *394*.